10th ECCOMAS Thematic Conference on Computational Methods in Structural Dynamics and Earthquake Engineering M. Papadrakakis, M. Fragiadakis (eds.) Rhodes Island, Greece, 15-18 June 2025

THE SEISMIC RESPONSE OF MOMENT FRAME BUILDINGS CONSIDERING THE GRAVITY CONNECTION TYPE

ARAN NASERPOUR¹, and AHMED ELKADY²

¹ University of Southampton, United Kingdom Burgess Road, Boldrewood Innovation Campus, Southampton SO16 7QF, UK a.naserpour@soton.ac.uk

² University of Southampton, United Kingdom Burgess Road, Boldrewood Innovation Campus, Southampton SO16 7QF, UK a.elkady@soton.ac.uk

Abstract

Past studies investigated the seismic response of steel moment frame buildings, considering the contribution of the gravity framing system. Although limited, these studies noted the potential role of the gravity framing system in preventing/delaying story mechanism formation and mitigating story drifts along the building height. In these studies, the numerical behavior of the gravity framing connections was either parametrically represented or calibrated based on limited test data for specific connection types. The present study evaluates the influence of gravity framing considering various semi-rigid connection types, including shear tab, flush endplate, and header plate connections. Recently developed accurate phenomenological models are employed for that purpose. These models can capture the various degradation mechanisms and ductility of semi-rigid connections under cyclic loading as a function of their geometry. A 4-story archetype building is investigated under static pushover and nonlinear response history analyses. The effect of the gravity connection type -and the gravity system as a whole- on the stiffness, strength, and ductility is quantified. The study shows that the effect of the gravity framing system strongly depends on the employed gravity connection. It is concluded that flush endplates are the most favorable in reducing drifts and residual drift ratio. These benefits can be realized without imposing further construction costs. The results highlight the potential of incorporating the gravity framing effect as part of the design procedure as well as analysis procedures, where ignoring them can be highly conservative.

Keywords: Gravity Framing, Semirigid Connections, Steel Moment Frames, Seismic Performance, Collapse Capacity.

1 INTRODUCTION

Steel moment-resisting frames are commonly assigned to the building's perimeter in North American design practice. This approach provides distinct advantages, such as simplifying construction and reducing material use under lateral loading. The gravity framing system (GFS) in this type of structure is typically designed with shear connections that are meant to support gravity loads. Those flexible connections are idealized as pinned in structural analysis and are consequently ignored in structural simulations.

Several gravity connections are used in construction practice, such as flush endplates (FEPCs), header plate (HEPCs), double web angle (DWACs), and shear tab connections (STCs). Laboratory tests revealed that FEPCs exhibit appreciable flexural capacity, reaching up to 32% of the plastic flexural capacity of the connected beam $(M_{\rm p,b})$ [1]. STCs can also develop notable flexural strength, up to 15% $M_{\rm p,b}$ [2]. Consequently, due to its nontrivial inherent lateral stiffness and strength, the GFS can act as a complementary backbone system to the main lateral force-resisting system. Early research identified GFS as a "backup system" that prevents collapse during earthquakes, as evidenced by the 1994 Northridge earthquake, where gravity framing stabilized buildings despite brittle beam-to-column connection failures [3-5]. It was shown that continuous gravity columns enhance structural robustness by increasing base shear capacity by 50%, collapse margin ratios by 40%, and preventing story-collapse mechanisms through increased flexural stiffness and resistance [1-4, 6, 7]. Gupta and Krawinkler [8] demonstrated that gravity frames improve structural response, but this is influenced by factors such as connection properties, column orientation, and drift demand. It is shown that stronger (semi-rigid) connection types can increase the building overstrength but reduce its ductility [6].

From a construction perspective, flush endplate, shear tab, and header plate connections are favored for their ease of fabrication, reduced material use, and faster installation, making them more cost-effective than fully rigid connections. Shear tab connections require minimal welding, while flush endplates and header plates offer moderate moment resistance with straightforward assembly. Their simpler detailing and reduced labor costs make them practical choices for projects, where full rigidity is not essential.

It is shown in previous research that the use of gravity framing systems has significantly improved the seismic performance [1, 6, 9]. However, past system-level performance assessments of MRFs have been conducted using idealized moment-rotation relationships for the gravity framing connections that were derived from the limited number of experimental results or the finite element models with special configurations. The main drawback of this approach, other than issues related to stiffness and strength accuracy, is overlooking rotational ductility [10].

This study delves deeper into this topic by examining how the gravity connection type influences the seismic performance (stiffness, strength, ductility, and collapse capacity) of steel MRF buildings. For this purpose, a 4-story building is investigated while employing accurate numerical models to capture the hysteretic response of STCs, HEPCs, and FEPCs up to failure.

2 ARCHETYPE BUILDING DETAIL

A 4-story archetype office building located in downtown Los Angeles, California (Risk category II, Importance factor, I_e =1, and soil class D) is investigated. The building is designed per ASCE7-16 [11-13], AISC 360-16 [14], and AISC 341-16 [15]. The building has a square plan, as shown in Figure 1, with 3-bay special moment frames (SMF) allocated along the pe-

rimeter. The SMF is designed with fully rigid Reduced Beam Sections (RBS) connections per AISC 358-16 [16]. The beam and columns are fabricated from steel ASTM A992 Gr. 50. The SMF columns are spliced at the mid-height of odd-numbered stories, except for the first story. The dead and live loads on the typical floor are taken as 4.31 and 2.4 kN/m², respectively, while the roof live loads are considered 0.96 kN/m². The cladding loads are taken as 1.2 kN/m². For the GFS, the beam and column sections are W16x45 and W12x65, respectively. The column section is kept constant along the height. The GFS connections are designed using three connection types: conventional STC, HEPC, and FEPC. The connection endplates are fabricated from grade A36 steel and A325 bolts where the threads were not excluded from the shear plane. All connections are designed with 4 M16 bolts. Figure 2 shows the engineering detail drawings for the three gravity connections.

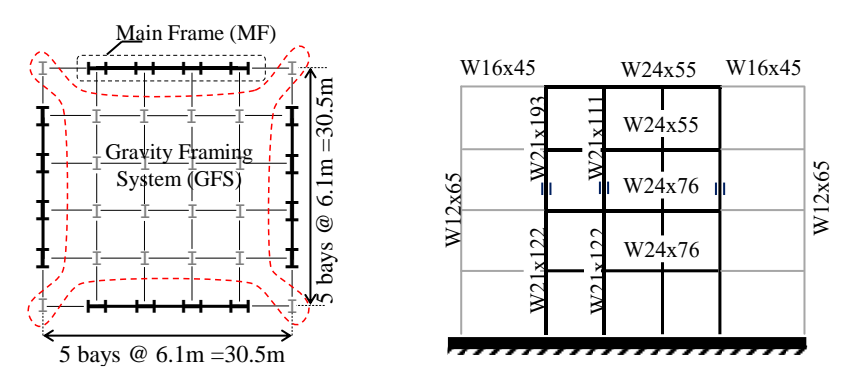


Figure 1: Plan and elevation of the 4-story steel moment frame.

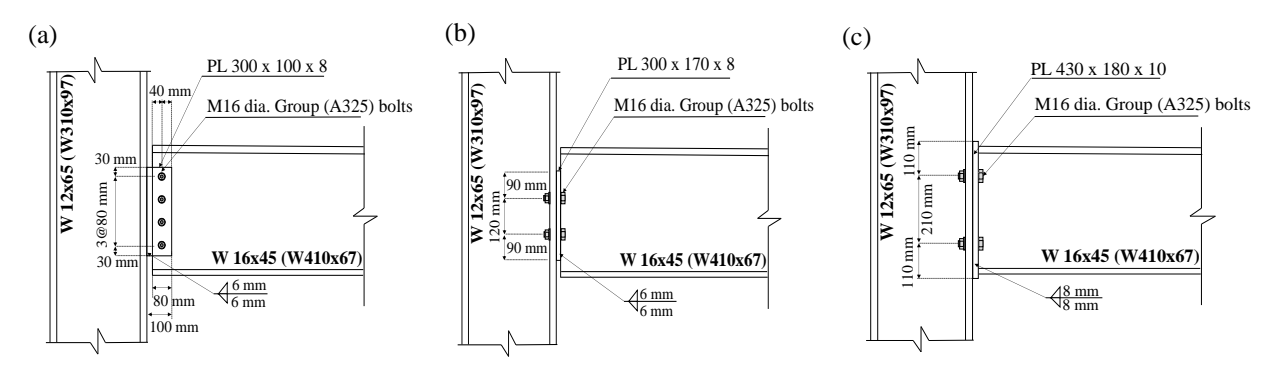


Figure 2: Detail of the gravity connections: a) STC; b) HEPC; and c) FEPC.

3 NUMERICAL MODEL CONFIGURATION

Two-dimensional numerical models are developed within the *OpenSees* simulation platform [17]. Four models are generated; one represents the bare steel perimeter SMF without consideration of the GFS (noted as B model), and the remaining three consider the GFS with the different gravity connection types (noted as BG_{STC}, BG_{HEPC}, and BG_{FEPC}). Note that the columns in the GFSs are considered with weak-axis orientation.

The models are built and analysed within the open-source software *FM-2D* [18]. The models employ the concentrated plasticity approach, where the beams and columns are idealized as elastic beam-column elements with nonlinear rotational springs at their ends, as illustrated in Figure 3. For the MRF springs, the phenomenological *IMKBilin* model is used [19], where its backbone and cyclic parameters are defined following the recommendation by Lignos and Krawinkler [20] for steel beams with RBS and by Lignos et al. [21] for wide-flange columns. The column panel zone is idealized using the mechanical parallelogram model [22] with the

Hysteretic model and the shear force-shear distortion parameters recommended by Skiado-poulos et al. (2021) [23]. For the STCs, HEPC, and FEPC, the springs are assigned either the phenomenological *Pinching4* or the *IMKPinching* models, whose backbone and cyclic deterioration parameters are calibrated based on continuum finite element (FE) simulations for the designed connections. The HEPC and STC spring models consider the beam edge binding on the column face at large rotations. To simulate this flexural strength stiffening effect, the *ElasticPPGap* model is used in parallel.

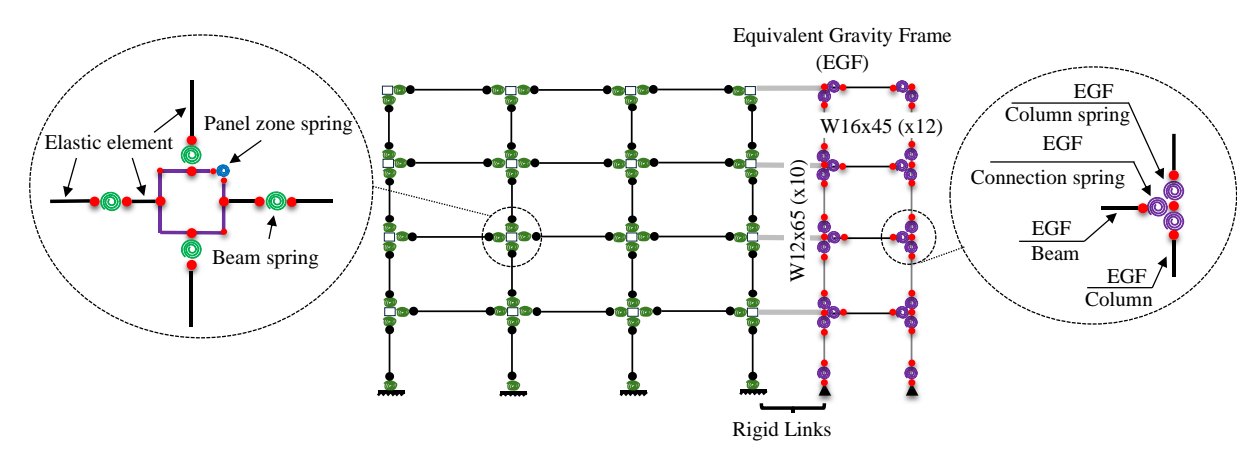


Figure 3: Illustration of 2-dimensional numerical idealization of the MRF and EGF models.

Referring to Figure 4(a), The STC achieves a flexural capacity ($M_{\rm max}$), approximately 4% $M_{\rm p,b}$ before bolt failure. At around 8% rotation, the bolt at the top row fails in shear, resulting in a sudden 50% strength drop. This is followed by beam edge binding, which causes a flexural strength stiffening to about $0.86M_{\rm max}$. The STC can undergo substantial deformations, reaching up to 14% radians before complete failure. The HEPC reaches a flexural strength of 6% $M_{\rm p,b}$ at 8% radians (see Figure 4(b)). After this point, due to the beam-binding effect, the flexural strength is almost doubled. Finally, the FEPC exhibits the largest $M_{\rm max}$) equal to 17% $M_{\rm p,b}$ (see Figure 4(c)). After tension bolts (top row) failure at 8% radians, the connection retains residual resistance of about 23% $M_{\rm max}$), driven by endplate bending and supported by the compression bolts (bottom row). This residual moment can be maintained even at extremely large rotations; however, a 20% radians limit is proposed herein for practical purposes. Note that coincidently, excluding the beam-to-column binding phase, all three connections achieved their maximum capacity around 8% rotation. Based on CEN [24] classification criteria, the STC and HEPC are classified as pinned connections. However, the FEPC is classified as a semi-rigid connection.

A fictitious one-bay frame, referred to as the equivalent gravity frame (EGF), is employed to capture the building's *P-delta* forces and the GFS contributions. The EGF is connected to the main frame with the gravity frame by axially rigid truss links as defined and described in [8, 25, 26]. A two percent damping ratio (ξ =2%) is considered at the first and third modes. The stiffness-proportional term in Rayleigh damping is exclusively applied to the elastic column and beam elements, while the mass-proportional term is allocated to all frame nodes with associated masses [27].

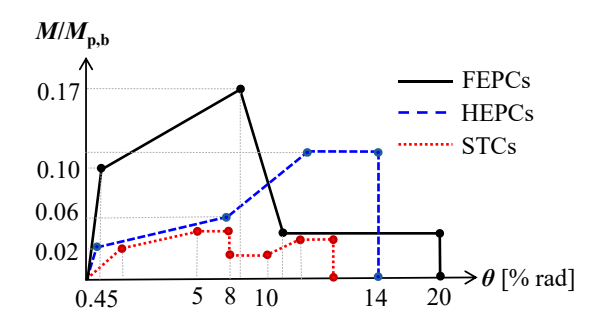


Figure 4: The normalized M- θ relationship of STCs and FEPCs.

4 PERFORMANCE ASSESSMENT

4.1 Fundamental mode period

The first-mode periods (T_I) for all models are summarized in Table 1. Based on this table, when gravity framing is incorporated into the analytical models, the lateral stiffness of the archetype building increases. Consequently, the computer-based period of each archetype building decreases by approximately 1%, 4%, and 6% for BG_{STC}, BG_{HEPC}, and BG_{FEPC} compared with the bare steel models only, respectively. This demonstrates that the FEPCs contribute to a greater increase in the stiffness of the archetype MRF compared to other connection types. Note that in previous research [1], the decrease in the period of the 4-story buildings with STC in GFS (i.e., as a semi-rigid connection) was 8% due to the semi-rigidity class of considered connections. For reference, the code-based period [28] is 0.685s, which is almost half the computer-based one.

4.2 Static pushover response

Figure 5 shows the static pushover responses (base shear force versus the roof drift ratio), considering the first mode pattern. In Figure 5, the base shear is normalized by the building's seismic weight (W_s). The BG_{STC}, BG_{HEPC}, and BG_{FEPC} case models experiences around 4%, 8%, and 18% increase in the base shear strength of, compared to the bare steel models. This is further assessed by quantifying the static overstrength (Ω_s) and period-based ductility factor (μ_T) as defined in [29] and summarized in Table 1. The static overstrength is dependent on the period of the frames. The static overstrength for the BG_{FEPC} is approximately 20% higher than the B. This suggests that the currently specified overstrength for SMFs (Ω_0 =3) as per [28] is over-conservative. This observation is consistent with previous analytical and numerical research [9, 29-32].

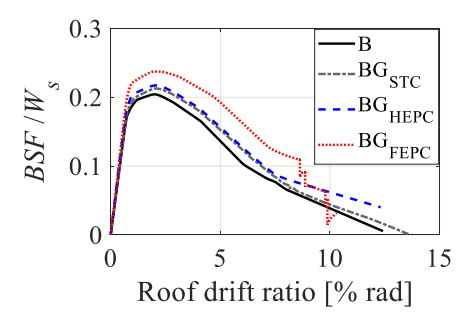


Figure 5: Pushover curves of the 4-story building with/without GFS effect.

Concerning ductility, the BG_{STC}, BG_{HEPC}, and BG_{FEPC} models achieve higher μ_T values than the B model (4%, 5%, and 15%, respectively). The largest μ_T is associated with the

 BG_{FEPC} case due to the higher ductility in the hardening region compared to other connections. The shear failure of the 1^{st} bolt row in STCs decreases the period-based ductility in comparison with the BG_{FEPC} case.

Case	$T_1[s]$	Ω_s	Ω_d	μ_T
В	1.22	1.95	2.70	5.10
BG _{STC}	1.21	2.06	2.85	5.26
BGHEPC	1.17	2.14	3.10	5.28
BGFEPC	1.15	2.33	3.20	5.90

Table 1: Computer-based period, static overstrength, and period-based ductility of the building.

4.3 Dynamic response at DBE and MCE intensities

Nonlinear response-history analysis (NRHA) is carried out using the far-field ground motion record suite specified in [29]. The records were scaled to two target seismic intensities, the design-based earthquake (DBE) and maximum considered earthquake (MCE) intensity. Table 1 shows the dynamic overstrength Ω_d of the 4-story steel building. As expected, Ω_d is larger than Ω_s . It is concluded that the higher mode contribution to dynamic redistribution of shear forces causes this difference compared to those derived from conventional lateral load patterns commonly used in pushover analysis [1, 25, 33, 34]. It seems that for the 4-story archetype building in this paper, the dynamic overstrength factor shows sensitivity to GFS connection strength.

Figure 6 compares the median story drift ratio (*SDR*), residual drift ratio (*RDR*), and peak floor acceleration (*PFA*) at the MCE intensity. Lower drifts are observed when the GFS is considered. The *SDR* at the roof decreased by 20% and 11% for the BG_{FEPC} and BG_{HEPC} models at DBE intensity compared to the bare SMF. This reduction is about 25% at the MCE level when using FEPCs. This confirms the potential role of the GFS as a backup/backbone system, conditional on the utilization of a gravity connection with appreciable capacity.

Similarly, the *RDR* is consistently reduced in all stories. FEPCs demonstrate strong potential as GFS connections, offering higher performance by reducing *RDR* 60% and 55% at DBE and MCE, respectively. This is key for maintaining post-earthquake functionality. This rate for BG_{HEPC} is 10% in DBE level. At the MCE level, the GFS presence leads to a reduction in *PFA* in the middle floors (7%, 10%, and 12% for BG_{STC}, BG_{HEPC}, and BG_{FEPC}). This means that damage in acceleration-sensitive non-structural components (e.g., suspended ceilings, mechanical and electrical systems) is, in reality, lower than what would be expected if only the SMF is considered.

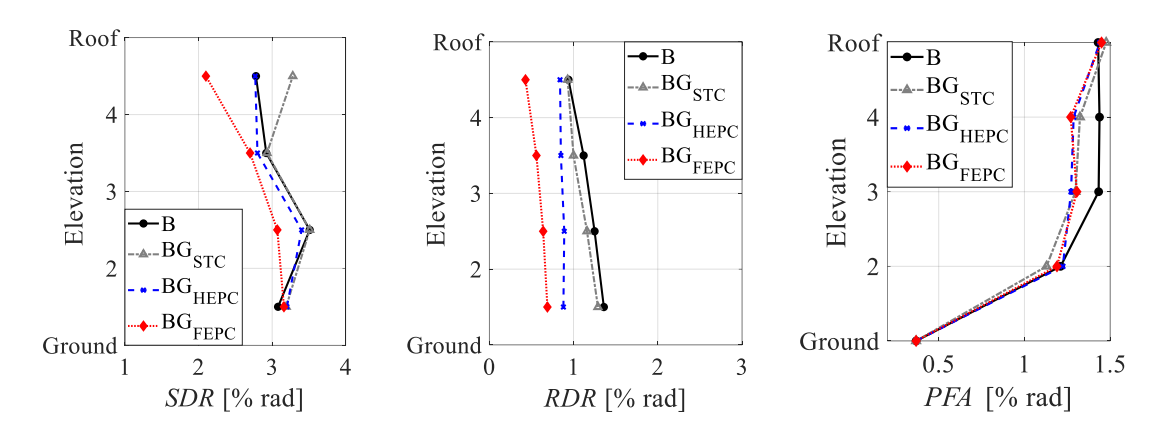


Figure 6: Median SDR, RDR, and PFA profiles at MCE intensity.

4.4 Collapse capacity

The collapse capacity of the building is investigated through incremental dynamic analysis. The collapse fragility curves (i.e., fitted lognormal cumulative distribution curves) are compared in Figure 7. The models with GFS demonstrate an average 30% increase in the median collapse intensity compared to the B model. As expected, GFSs with FEPCs reach 20% and 13% more collapse capacity than BG_{STC} and BG_{HEPC}. It is worth noting that the record-to-record variability values remain relatively consistent across all analytical models, indicating that while gravity framing enhances collapse resistance, they have little effect on the variability of seismic response, at least for the studied 4-story building [1].

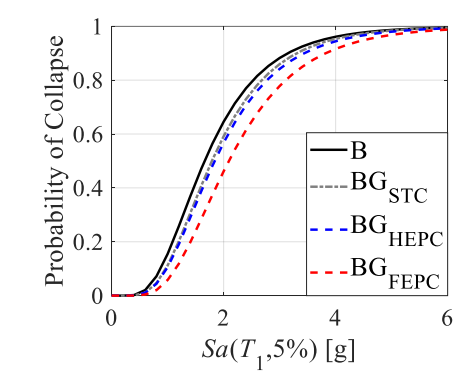


Figure 7: Collapse fragility of archetype building with various GFS connections

5 CONCLUSION

This study investigated the influence of gravity-framing systems (GFS) with various connection types on the seismic performance of steel moment frame buildings. Three common gravity connections are employed: shear tab (STC), header plate (HEPC), and flush endplate connections (FEPC). Using static and dynamic analysis, the effect of GFS and the connection type on a 4-story archetype building is evaluated. The key findings are as follows:

• Gravity framing systems, especially those with FEPCs, reduced median story drift ratios (*SDR*) by 20% and residual drift ratios (*RDR*) by 60% across all floors at the design-basis earthquake intensity, highlighting the importance of gravity framing in improving post-earthquake repairability.

- The static overstrength and period-based ductility of the building were significantly influenced by the GFS. Models incorporating gravity framing exhibited higher overstrength factors (~6%, 10%, and 20% for GFS with STCs, HEPCs, and FEPCs, respectively) and ductility (~15%). FEPCs demonstrated superior performance in terms of overstrength.
- The GFS connection type plays a critical role in the building's collapse capacity. FEPCs were found to be the most effective in increasing the collapse capacity by 30%. STCs and HEPC also provided benefits but were less effective (about 10% increase) compared to FEPCs.

In conclusion, this study corroborates the critical role of gravity framing systems in enhancing the seismic performance of steel moment frame buildings. The type of gravity connection significantly influences the structural response, with flush endplate connections emerging as the most favourable option based on this short study.

REFERENCES

- [1] A. Elkady, D.G. Lignos, Effect of Gravity Framing on the Overstrength and Collapse Capacity of Steel Frame Buildings with Perimeter Special Moment Frames, *Earthquake Engineering & Structural Dynamics* 44(8) (2015) 1289–1307.
- [2] J. Liu, A. Astaneh-Asl, Moment-Rotation Parameters for Composite Shear Tab Connections, *Journal of Structural Engineering* 130(9) (2004) 1371-1380.
- [3] R.T. Leon, Semi-rigid composite construction, *Journal of Constructional Steel Research* 15(1) (1990) 99-120.
- [4] R.T. Leon, D.J. Ammerman, Semi-rigid composite connection for gravity loads, *Eng. J.* 27 (1990) 12.
- [5] R. Tremblay, S. Stiemer, Back-up stiffness for improving the stability of multi-storey braced frames under seismic loading, (1994).
- [6] F.X. Flores, F.A. Charney, D. Lopez-Garcia, Influence of the Gravity Framing System on the Collapse Performance of Special Steel Moment Frames, *Journal of Constructional Steel Research* 101(0) (2014) 351-362.
- [7] M. Del Carpio Ramos, G. Mosqueda, M. Javad Hashemi, Large-Scale Hybrid Simulation of a Steel Moment Frame Building Structure through Collapse, *Journal of Structural Engineering* 142(1) (2016) 04015086.
- [8] A. Gupta, H. Krawinkler, Seismic Demands for the Performance Evaluation of Steel Moment Resisting Frame Structures, The John A. Blume Earthquake Engineering Center, Stanford University, CA, 1999.
- [9] D.A. Foutch, S.Y. Yun, Modeling of Steel Moment Frames for Seismic Loads, *Journal of Constructional Steel Research* 58(5) (2002) 529-564.
- [10] Z. Ding, A. Elkady, Backbone Models for Partial-Strength Steel Endplate Connections, *Journal of Structural Engineering* (under review) (2025).
- [11] AISC, Seismic provisions for structural steel buildings, American Institute of Steel Construction2022.
- [12] AISC, Specifications for structural steel buildings. ANSI/AISC360-10, American Institute of Steel Construction (AISC), Chicago, 2022.
- [13] AISC, Prequalified Connections for Special and Intermediate Steel Moment Frames for Seismic Applications, American Institute for Steel Construction, Chicago, IL, 2022.

- [14] AISC, Specification for Structural Steel Buildings, American Institute for Steel Construction, Chicago, IL, 2016.
- [15] AISC, Seismic Provisions for Structural Steel Buildings, American Institute for Steel Construction, Chicago, IL, 2016.
- [16] AISC, Prequalified Connections for Special and Intermediate Steel Moment Frames for Seismic Applications, American Institute for Steel Construction, Chicago, IL, 2016.
- [17] F.T. Mckenna, Object-Oriented Finite Element Programming: Frameworks for Analysis, Algorithms and Parallel Computing, Department of Civil Engineering, University of California, 1997.
- [18] A. Elkady, FM-2D-open-source platform for the 2-dimensional numerical modeling and seismic analysis of buildings, *SoftwareX* 17 (2022) 100927.
- [19] L.F. Ibarra, R.A. Medina, H. Krawinkler, Hysteretic Models that Incorporate Strength and Stiffness Deterioration, *Earthquake Engineering & Structural Dynamics* 34(12) (2005) 1489-1511.
- [20] D.G. Lignos, H. Krawinkler, Deterioration Modeling of Steel Components in Support of Collapse Prediction of Steel Moment Frames under Earthquake Loading, *Journal of Structural Engineering* 137(11) (2011) 1291-1302.
- [21] D.G. Lignos, A. Hartloper, A. Elkady, G.G. Deierlein, R. Hamburger, Proposed Updates to the ASCE 41 Nonlinear Modeling Parameters for Wide-Flange Steel Columns in Support of Performance-based Seismic Engineering, *Journal of Structural Engineering* 145(9) (2019) 04019083.
- [22] H. Krawinkler, S. Mohasseb, Effects of panel zone deformations on seismic response, *Journal of Constructional Steel Research* 8 (1987) 233-250.
- [23] A. Skiadopoulos, A. Elkady, D.G. Lignos, Proposed panel zone model for seismic design of steel moment-resisting frames, *Journal of Structural Engineering* 147(4) (2021) 04021006.
- [24] CEN, Eurocode 3 Design of Steel Structures, Part 1-8: Design of Joints, European Committee for Standardization, Brussels, Belgium, 2005.
- [25] D.G. Lignos, C. Putman, H. Krawinkler, Seismic Assessment of Steel Moment Frames Using Simplified Nonlinear Models, *Computational Methods in Earthquake Engineering* 30 (2013) 91-109.
- [26] D.G. Lignos, C. Putman, F. Zareian, H. Krawinkler, Seismic Evaluation of Steel Moment Frames and Shear Walls Using Nonlinear Static Analysis Procedures, ASCE Structures Congress, 2011, pp. 2204-2215.
- [27] F. Zareian, R.A. Medina, A Practical Method for Proper Modeling of Structural Damping in Inelastic Plane Structural Systems, *Computers & structures* 88(1) (2010) 45-53.
- [28] ASCE, Minimum Design Loads ans Associated Criteria for Buildings and Other Structures, American Society of Civil Engineers, Reston, VA., 2016.
- [29] NIST, Evaluation of the FEMA P695 Methadology for Quantification of Building Seismic Performance Factors, NEHRP consultants Joint Venture, 2010.
- [30] S. Mehanny, P. Cordova, G. Deierlein, Seismic Design of Composite Moment Frame Buildings—Case Studies and Codes Implications, *Composite Construction in Steel and Concrete IV* (2002) 551-562.
- [31] J. Jin, S. El-Tawil, Seismic Performance of Steel Frames with Reduced Beam Section Connections, *Journal of Constructional Steel Research* 61(4) (2005) 453-471.
- [32] F. Zareian, D.G. Lignos, H. Krawinkler, Evaluation of Seismic Collapse Performance of Steel Special Moment Resisting Frames Using FEMA P695 (ATC-63) Methodology, ASCE Structures Congress, Orlando, Florida, USA, 2010, pp. 1275-1286.

- [33] D.G. Lignos, H. Krawinkler, A.S. Whittaker, Prediction and Validation of Sidesway Collapse of Two Scale Models of a 4-Story Steel Moment Frame, *Earthquake Engineering & Structural Dynamics* 40(7) (2011) 807-825.
- [34] B. Alavi, H. Krawinkler, Behavior of Moment Resisting Frame Structures Subjected to Near Fault Ground Motions, *Earthquake Engineering & Structural Dynamics* 33(6) (2004) 687-706.